A Survey of the Effects of Small Protuberances on Boundary-Layer Flows

RAYMOND SEDNEY
Ballistic Research Laboratories, Aberdeen Proving Ground, Md.

I. Introduction

CONSIDERING the vast amount of work that has been done in the general area of boundary-layer flows, it is remarkable that the following question has not received a great deal of attention. If a boundary layer over a smooth surface is subjected to a local, steady, small disturbance how does the flow respond? If the boundary layer is laminar it can be argued that most of the investigations of stability and transition are directed toward this question and that the answer is that, almost always, the flow will become turbulent; otherwise the disturbance will decay and the flow will return, asymptotically, to its undisturbed form. However several questions remain. What happens to the flow before transition occurs or how is the laminar, asymptotic form approached? What is the nature of the flow, shear stress, and heat transfer near the disturbance? Similar questions can be asked if the unperturbed boundary layer is turbulent. An understanding of such flows poses difficult theoretical problems which have been essentially untouched by analytical methods. But this understanding is required in such diverse applications as flow induced in the atmospheric boundary layer by terrain changes, e.g., an isolated hill or structure, or flow over aerodynamic vehicles. In practice, almost all vehicles have small protuberances such as connectors, lugs, rotating bands, etc. and, of course, large protuberances such as wings and fins. The flowfield in the neighborhood of these perturbations exemplifies strong viscous interaction in three dimensions; it is not surprising, then, that there has been little progress in theoretical work. Experimentally, flow visualization is mandatory to gain insight into the complex flow patterns.

The most commonly investigated disturbance in boundary layers is a protuberance on the surface. Whether or not the protuberance causes a small disturbance depends on whether we view it on the scale of the boundary layer or on the scale of the external flow. (Of course the small disturbance may grow with time or distance.) For the purposes of this survey a protuberance is small if its effect on the external flow is small. This implies that the dimension normal to the surface k is of the order of the boundary-layer thickness δ but the other dimensions are not restricted. Actually the data reviewed pertain to the case where the streamwise dimension is also of order δ. On the boundary-layer scale, if $k = 0(\delta)$, the perturbation will be large at least in the neighborhood of the protuberance; it may be small at downstream distances large compared with k. The purpose of this paper is to survey the available information on boundary-layer flow perturbations caused by small protuberances. This information is mainly experimental; from it the major elements of a flow model can be deduced. For large protuberances and supersonic external flows, Korkegi[2] has reviewed the pertinent data; these are mainly pressure and heat-transfer distributions and shock interaction phenomena.

Even when the protuberance is small there are a large number of parameters to consider: undisturbed boundary-layer profiles (2-D and 3-D) and thickness; dimension, position and shape of the protuberance; external velocity U and velocity u_k at the scale height k; various Reynolds numbers that can be formed from these quantities; Mach number; heat and mass transfer. Although the experimental evidence is still limited, it seems to indicate that the gross features of the flow are weakly dependent on variations of these parameters. The fact that a shear flow is being perturbed and the presence of the wall are significant features of the flow environment. Some of the scales of the perturbed flow are much smaller than the scale of the protuberance. For 3-D small protuberances the data show that a number of common elements exist in the disturbed flow regardless of whether the boundary layer is laminar or turbulent, the speed range of the external flow, or the detailed shape of the protuberance. 1) In the upstream separated flow a system of vortices is formed. 2) These are stretched around the protuberance in a horseshoe vortex fashion and persist as streamwise vortices far downstream. 3) Spiral vortices rise up from the surface in the near wake. The details of the downstream disturbance depend on whether or not transition takes place in a laminar boundary layer.

For an isolated roughness or protuberance in a laminar boundary layer some general conclusions can be summarized as follows. For low-speed flow, if the roughness height k is small compared to δ, and the freestream velocity small enough, early transition does not occur but the disturbance persists for downstream distances of hundreds of roughness heights. For high-speed flow, even if k is comparable to δ, transition may not occur although the flowfield is considerably distorted far downstream of the roughness. In both cases even if transition does

Raymond Sedney is Chief of the Fluid Dynamics Research Group in the Exterior Ballistics Laboratory of B.R.L. He was with the Martin-Marietta Corp. in the Baltimore Division from 1966 to 1967 and in the R.I.A.S. Division from 1967 to 1971. From 1953 to 1966 he was at B.R.L. and spent the previous two years with the Douglas Aircraft Co. He received the D.Sc. (1951) and M.S. (1950) in applied mathematics and B.S. in physics (1948) from the Carnegie Institute of Technology. He has been a member of the AGARD Fluid Dynamics panel and is currently serving on the AIAA Technical Committee on Fluid Dynamics; he is an Associate Fellow of the AIAA.

Presented as Paper 72-713 at the AIAA 5th Fluid and Plasma Dynamics Conference, Boston, Mass., June 26–28, 1972; submitted July 25, 1972; revision received December 27, 1972. Some of this work was done while the author was with the R.I.A.S. Division, Martin-Marietta Corporation where it was partially supported by the Army Research Office—Durham. An earlier review, but of more limited scope, is available in Ref. 1.

The author would like to dedicate this paper to the memory of M. H. Bertram, Head, Hypersonic Aircraft Fluid Mechanics Branch, NASA Langley Research Center.

Index categories: Boundary Layers and Convective Heat Transfer—Laminar; Boundary Layers and Convective Heat Transfer—Turbulent; Boundary-Layer Stability and Transition.

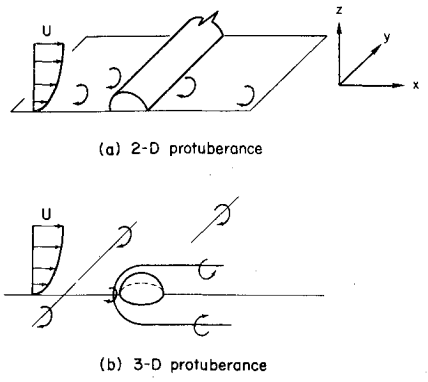

Fig. 1 Sketch showing the behavior of vortex lines for 2-D and 3-D flow. Definition of coordinate system.

occur there can be extended regions where the flow is relatively steady but certainly distorted. Thus, although transition provides some of the motivation for the subject of this work and transition studies supply the experimental background, this paper is not one on laminar-turbulent transition. Also stability of laminar flows in the classical sense is not treated. Thus transition will be mentioned often in the subsequent discussion, but it would be out of place to dwell on that topic. There have been several reviews of transition lately: for low-speed flow by Tani[3,4] and for high-speed flow by Morkovin[5] and Henderson.[6] These contain some discussion of the effect of isolated 2-D and 3-D roughness elements (see especially Ref. 5). Obviously we expect the distortion in the flowfield to be different for the 2-D and 3-D types of disturbance. It is not so clear how transition is affected since it is known that the development of 3-D disturbances, of the type discussed by Lin and Benney[7] and the associated streamwise vorticity are necessary in order for transition to develop beyond the stage described by the classical 2-D linear stability theory (see Stuart[8] for a discussion of this). The 3-D nature of the flows discussed here is distinct from that considered by Lin and Benney[7] in their model of the nonlinear stability problem, the 3-D disturbance is assumed to be present because of the inevitable departure from 2-D conditions in any real flow. For the flow discussed in this paper three-dimensionality is induced by a steady perturbation in an otherwise 2-D boundary layer.

It would be more conventional to take up the 2-D problem first. Certainly any analysis would be much simpler than for the 3-D case but its utility is questionable. It is always difficult to realize experimentally an approximation to steady 2-D flows. It is especially difficult in perturbed boundary layers because the relatively low inertia of the fluid near the wall makes that region very susceptible to small pressure gradients in the cross-stream direction. Most of the experiments involving a 2-D roughness element have been concerned with the gross effects on transition and correlations of the data with little regard to the departure from two-dimensionality. A number of analytical attempts have been made to examine some limited portion of the flow; these will be summarized later. Although these papers have interest in their own right the restriction to 2-D flow is a fundamental one; a 3-D perturbation is not just more difficult to describe analytically but different physical processes take place.

The physical explanation of the major differences in the two cases is relatively straightforward to understand in terms of the behavior of vorticity. Consider a 2-D boundary-layer flow over a surface that is smooth except for the presence of a small bump. Upstream of the bump the flow has vorticity in the y-direction (see Fig. 1). If the bump is 2-D, Fig. 1a, then the vorticity remains fixed in that direction; it is convected downstream and, except for viscous diffusion, the vorticity carried by each vortex line would remain constant. If the bump is 3-D, Fig. 1b, the vortex lines must be stretched as they pass over and around the obstacle, vorticity is concentrated near the stagnation point, and a streamwise (x) component of vorticity is induced. This x-component of vorticity causes some of the interesting and important effects for 3-D perturbations. Vorticity stretching is, of course, independent of viscous effects since it is represented by the first term on the right-hand side of the vector equation

$$D\boldsymbol{\omega}/Dt = (\boldsymbol{\omega}\cdot\nabla)\mathbf{v} + \nu\nabla^2\boldsymbol{\omega}$$

where $\boldsymbol{\omega}$ is vorticity, $\mathbf{v}$ is velocity and ν is kinematic viscosity There have been several analytical investigations of flow over bodies immersed in an inviscid shear flow; Leibovich and Koh[9] give a fairly complete list of references. Neglecting viscous effects is a reasonable approximation for some aspects of flow over a body immersed in a boundary layer if the body is not close to the wall, see Lighthill.[10] As the body approaches the wall, viscous effects will become important. For the case of a 3-D protuberance in a boundary layer, vorticity stretching, concentration of vorticity in front of the protuberance, streamwise vorticity, and viscous effects must all be considered.

We are thus confronted with a formidable problem; but if the protuberance is small we should expect some simplification since it should have only a local effect on the pressure gradient. Thus, for a small protuberance, it should be possible to consider the problem in two parts; the flow in the neighborhood of the protuberance and the flow downstream. Examination of the pertinent experimental data seems to support this expectation. Unless the shape of the protuberance satisfies rather rigid requirements, the boundary-layer approximation will fail in the neighborhood of the disturbance and in an elongated region downstream. At some distance downstream the boundary-layer approximation can again be applied using the undisturbed pressure gradient. The initial conditions, determined from the local solution, will contain streamwise vorticity, i.e., cross flow.

The resulting 3-D boundary-layer problem is of a type that has not received much attention. Suppose the surface is a flat plate and that the 3-D boundary layer develops in the absence of pressure gradients, the cross flow appearing because of the initial conditions. From this it is evident that a correction to a general theorem in 3-D boundary-layer flows, Sedney[11] and Squire,[12] must be made. (The incomplete form is given in Rosenhead,[13] p. 457.) To have zero cross flow it is not sufficient for the inviscid streamlines to be geodesics of the surface; it is also required that an initial profile with zero cross flow be given. There are some other questions which arise from the small protuberance problem but have more general interest: If a boundary layer in which streamwise vorticity or cross flow has been generated is allowed to relax under zero cross-stream pressure gradient, does the cross flow always decay? If so in what manner? What effect does a streamwise pressure gradient have on the decay? etc. Apparently these questions have not been treated in the literature. Such questions can be classified as part of the initial value problem of boundary-layer theory. Some results are discussed in the last section; but it should be emphasized that these and other analytical results are far from providing a solution to the perturbation problem.

There are other means of generating a steady, local disturbance in boundary layers, e.g., impingement of a jet, wake, or shock wave. Although each of these will have special features, some elements of the perturbed flowfields will be similar to those of the protuberance. Only the latter will be considered in the review of experimental data presented here.

II. Review of Experimental Data

Most of the experimental work concerned with small protuberances or roughness elements as disturbances in boundary layers gives the over-all results on transition. Specifically, correlations of a transition Reynolds number with k/δ_k^* or with the local roughness Reynolds number, $Re_k = u_k k/\nu$, are given; here δ_k^* is the undisturbed boundary-layer displacement thickness at the position of the roughness, u_k is the undisturbed velocity at height k off the surface, and ν is the kinematic viscosity. This large body of literature will not be mentioned

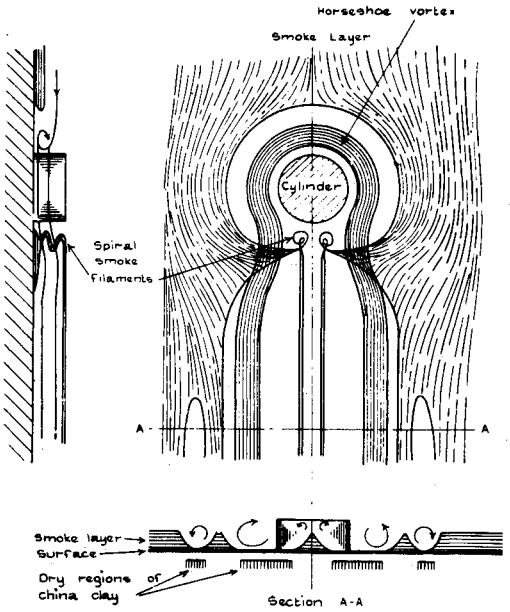

Fig. 2 Sketch of flow past a protuberance in a boundary layer. From Ref. 16 (see also Ref. 17).

since the purpose here is to review the work that gives information on the details of the disturbed flowfield.

1. Low-Speed Flow

a) *Laminar flow:* Most of the detailed probing of the flowfield has been done for low-speed flow. When the flow is laminar, the highly developed art of visualizing the flow by the smoke technique can be used; this gives the most insight into the 3-D flow patterns. Often in the following we shall need to refer to distances measured from the streamwise position of the protuberance, x_k, in terms of protuberance height, k, i.e.,

$$X \equiv (x - x_k)/k$$

For 2-D protuberances there are two papers that give information on the disturbance to a flat-plate boundary layer caused by a cylindrical rod. Tani and Sato[14] give rather limited data whereas Klebanoff and Tidstrom[15] give considerably more. Qualitatively both agree on the nature of the perturbed flow and nothing unexpected is found. Reference 15 reports upstream influence caused by the rod which extends to $X = -30$ for $k/\delta_k{}^*$ varying between 0.71 and 0.85 and Re_{x_k} varying between 2×10^5 and 2.84×10^5. Presumably the flow is separated in this region but Ref. 15 is not definite on this point; the measured velocities are always less than those for the undisturbed flow. Downstream the flow is separated, the height of the reversed flow region never exceeding k. Reattachment occurs for X between 30 and 40 in Ref. 15, for the same parameter as quoted previously, with some dependence on unit Reynolds number. The recovery zone extends to $X \cong 70$ with slight dependence on unit Reynolds number. This zone is defined as "the region between the roughness element and the recovery position, where the recovery position is the downstream position at which the mean velocity profile has returned to the type of distribution that it would have without the roughness." Transition occurs beyond the recovery position for the data quoted here. For $Re_{x_k} = 2.3 \times 10^5$ the beginning of transition is at $X = 290$ although "spikes" are observed in the velocity fluctuation data somewhat upstream of this. Examination of the fluctuation data, which is the main point of Ref. 15, shows that "upstream of breakdown highly concentrated discrete vortices are not present." The data of Ref. 14 are more limited. Only one case is given where transition occurs beyond the recovery zone. For $k/\delta_k{}^* = 0.45$ and $Re_{x_k} = 6.7 \times 10^5$, reattachment occurs at $X = 80$ and the recovery position is at $X = 220$. With $k/\delta_k{}^* = 1.9$ and the same Re_{x_k}, transition occurs in the separated flow and reattachment is then at $X = 12$. "Fully developed turbulent profiles are established soon after reattachment."

As to the degree of unsteadiness in the perturbed laminar flow, for the parameters quoted above for Refs. 14 and 15, the maximum intensity of the fluctuations was at most 1% of the external velocity. It is well known that a 2-D roughness element is generally more effective in promoting transition than a 3-D element of the same $k/\delta_k{}^*$ for low-speed flow. It can be conjectured that it is more likely to generate unsteadiness than a comparable 3-D roughness element.

Conjecture on this point is required because the papers on 3-D roughness to be reviewed now are not explicit on the degree of unsteadiness in the disorted flowfield.

Gregory and Walker[16] were apparently the first to give a systematic account of transition due to 3-D roughness elements and also to give a detailed description of the flowfield. This was visualized by the smoke and the china-clay techniques. The former is capable of showing "short-exposure" details whereas the latter gives an average over a long time. Although an attempt will be made to describe the most important flowfield details from this paper (and the following one), a true appreciation of the results of such flow visualization studies can be obtained only by observing the photographs in the original papers.

The main purpose of the work by Gregory and Walker was to investigate transition and the characteristic turbulent wedge that usually occurs behind a small 3-D protuberance. These two matters are not relevant to our purposes and will not be mentioned except for the following observation. For a flat plate (and also to some extent for a portion of an air-foil section with zero pressure gradient) the turbulent wedge appears first at some distance downstream of the roughness. For a fixed freestream velocity, as the height of the roughness, k, changes, the apex of the turbulent wedge gradually approaches the roughness element. For an airfoil the smallest possible increase in k, which was 0.001 in., "encompassed the change from twin streaks (to be described presently) to a fully turbulent wedge emanating from the pimple." Thus the effect of pressure gradient and/or surface curvature is to make for much greater sensitivity in the response of the flow to the 3-D disturbance.

These tests were made in a wind tunnel with speeds up to 120 fps with the china-clay visualization technique employed and in a low-speed smoke tunnel with speeds up to 16 fps. The roughness elements were a) cylinders with height equal to diameter, which varied from 0.007 in. to 0.020 in., b) 60° cone with adjustable height, c) some squat cylinders with k much less than the diameter, and d) in one case an irregular mound of Plasticine. In all cases $k \leqq \delta_k$. In general the resulting flowfield distortion did not change much with the shape of the roughness element but seemed to depend primarily on Re_k and Re_{x_k}.

The results are best described by quoting Gregory and Walker and by looking at Fig. 2 which is taken from their paper (see also Thwaites,[17] p. 554).

"The boundary layer produces a static pressure gradient along the front stagnation generator of the cylinder. There is consequently an inflow towards the plate and a reverse flow forwards along its surface. The fluid rolls up into a number of continuously-generated horseshoe-shaped vortices which are seen wrapped round the cylinder and trailing downstream as a multi-ply vortex pair with axes parallel to the direction of the main flow. The number of vortices in front of the pimple, all rotating in the same direction, depends on the speed of the flow; as many as three have been observed."

"The observations showed that the flow pattern and the manner of breakdown of the flow to turbulence changed with the Reynolds number of the experiment. At small Reynolds numbers, a pair of spiral smoke filaments were observed arising normally to the plate close behind the cylinder. On reaching the level of the top of the cylinder, the smoke filaments trailed

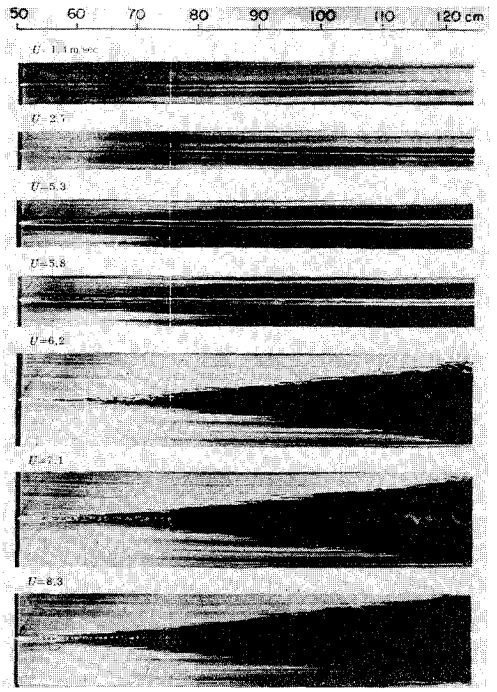

Fig. 3 Plan view of the flow induced by a spherical roughness element on a flat plate. The scale gives distance from the leading edge. Smoke is emitted on the plate downstream of the sphere; $x_k = 50$ cm, $k = 0.23$ cm. From Ref. 18.

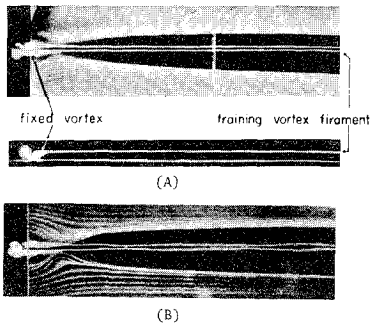

Fig. 4 Smoke visualization of the spiral and trailing vortices. A) Steady flow, plan and side views. B) Beginning of unsteadiness for slightly higher velocity. From Ref. 18.

downstream very close to each other along the centerline. As the wind speed was increased, a spreading turbulent wake appeared downstream of the cylinder, exhibiting a fine structure; the spiral filaments remained undisturbed. At larger Reynolds numbers, the horseshoe-shaped vortex appeared, wrapped round the front of the cylinder. At still larger Reynolds numbers, the twin vortex filaments leaving the top of the cylinder break down, and eddies are shed."

"An attempt was made to measure the frequencies with which the eddies were shed from the top of the pimple by observing the smoke stroboscopically. Precise measurements were not obtained, owing to unsteadiness in the flow and rapid diffusion of the smoke." The possibility was investigated of correlating this frequency, made nondimensional with u_k/k, with Re_k; scatter in the data precluded a definitive result.

The last quotation is their only comment on unsteadiness and it applied to the Reynolds number range for vortex shedding. At any rate there are conditions for which the flow is reasonably steady and has a consistent structure. No quantitative information is given on turbulence level in the tunnels.

For the smallest height of the conical protuberance (0.011 in.) and freestream speed of 120 fps, only a single streak was found in the china-clay but it is presumed there are really two which could not be resolved. Otherwise there was no significant change in the vortex patterns for the various shapes of roughness elements.

Typical values of the nondimensional parameters for which the vortex structure described above was observed are: $Re_{x_k} = 2.8 \times 10^5$, $Re_k = 150$, $k/\delta_k{}^* = 0.55$; over the region of observation the turbulent wedge did not appear for these parameters.

A remarkably detailed study of the flowfield behind spherical roughness elements was made by Mochizuki[18] using smoke for visualization. In general the results of Gregory and Walker described previously were verified; in addition many more details were discovered in the vortex patterns downstream of the roughness. In some cases both short and long exposure photographs were made. The spherical roughness was mounted on a flat plate and the tunnel flow adjusted for zero pressure gradient. Four values of k were used: 0.23, 0.33, 0.55, and 0.71 cm, and the sphere was placed at various distances from the leading edge of the plate. Besides injecting the smoke on the plate surface, the height of injection above the surface and its streamwise position were varied; plan and side views of the smoke patterns were photographed. The freestream speed was varied in small increments from 0.9 m/sec up to 8.3 m/sec.

For the smallest freestream speed, 0.9 m/sec, "only a reversed flow of smoke close behind the sphere and a single streak trailing downstream from it were observed;" no information is given on the resolution limit. The only significant difference between Mochizuki's observations and those of Ref. 17 is that the former says the spiral vortices and horseshoe vortex appeared at the same time.

Three of the photographs from Ref. 18 are reproduced here in Figs. 3–5. They illustrate several of the features found in Ref. 17 and described above. The results shown in Fig. 3 for $U = 5.3$ m/sec are particularly interesting; the parameters correspond closely to those in the experiments of Ref. 19, to be described shortly, in which quantitative results are given. The trailing vortex pattern remains steady and distinct at least for $X = 300$. For this case $k/\delta_k{}^* = 1.1$. This is shown more clearly in Fig. 4 which also illustrates that a slight increase in velocity (Ref. 18 does not specify the amount) causes periodic deformation of the trailing vortex. The structure of the horseshoe vortex pattern is further clarified in Fig. 5 where the smoke is injected upstream. This also shows vividly that what one sees in the visualization depends critically on how and where the smoke

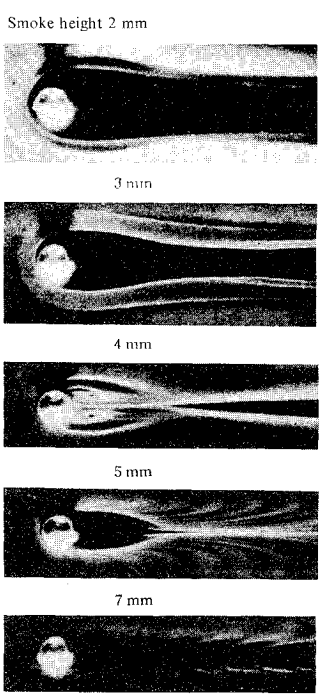

Fig. 5 Structure of the horseshoe vortex pattern illustrated by varying the height of upstream smoke injection, $k = 0.71$ cm. From Ref. 18.

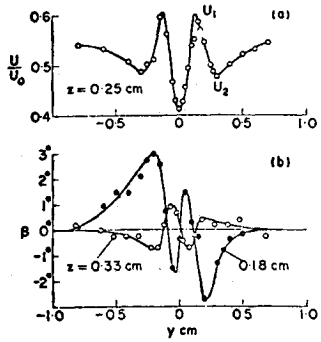

Fig. 6 Spanwise distribution of a) mean velocity in the x direction and b) flow inclination in the x-y plane at a fixed height off the surface. $k = 0.25$ cm, $x_k = 60$ cm, x-$x_k = 2.5$ cm, $\delta_k^* = 0.23$ cm and freestream velocity $U_0 = 5.2$ m/sec. From Ref. 19.

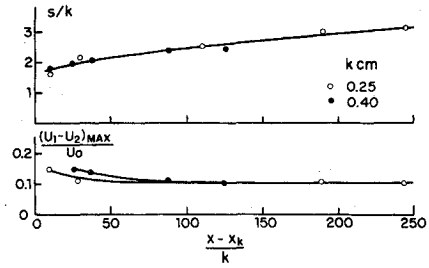

Fig. 8 Variation in streamwise direction of spacing of, and maximum velocity difference caused by, horseshoe vortex. $x_k = 60$ cm, $U_0 = 5.2$ m/sec. From Ref. 19.

is introduced. The near wake of the sphere is devoid of smoke except when it is injected at $z = 0.75k$. This implies that the near wake is fed by the upstream flow as first pointed out by Morkovin.[20]

Reference 18 also identifies an arch-shaped vortex pattern further in the wake. Several beautiful pictures are given illustrating the development of these. The height of the arch-shaped vortices was observed to increase rapidly near the sphere, so much that the tops were outside the boundary layer; but further downstream these vortices ceased to grow and gradually diffuse. This latter observation tends to indicate the boundary-layer nature of the downstream flow. Also periodic (in space) deformation of the horseshoe vortex, induced by the arch-shaped vortices, was observed. An attempt to make a quantitative correlation of the appearance of different features of the flow pattern in terms of k/δ_k and Re_k was partially successful.

Confidence in these visual studies is enhanced by the fact that the transition Reynolds number correlation with Re_k agrees with that obtained by others using hot wire anemometers; the visual definition of the transition point was taken as the vertex of the turbulence wedge whereas the hot wire studies used the point where the intermittency factor was 50%.

Morkovin[20] has pointed the way to a better understanding of these complex flowfields by classifying a series of "flow modules." For the protuberance in a boundary layer these are: the horseshoe vortex system, the lateral vortex sheets, the top vortex sheet, and the base flow-through module. Depending on the shape and size of the protuberance and the boundary layer in which it is immersed, these modules interact weakly to produce the patterns described above. The base flow-through module is particularly intriguing. The near wake is fed by the upstream flow and emptied by the spiral vortices. "The entrance appears to be generally through a low-lying area just upstream of the narrowest 'neck' of the flow viewed from above." This concept clarifies the role of the spiral vortices and represents a distinctly different concept from that of the customary 2-D separation with diffusion across dividing streamlines.

Some of the conclusions of Ref. 20 depend on the smoke visualization studies being carried on by R. Norman; the techniques he uses bring out more details in some parts of the flow than previous studies. For example, as many as seven vortices have been observed in the upstream separated flow. There is always an odd number; with five and seven, the "formations often tend to be 'burping' periodically."

The visual studies of Ref. 18 are nicely complemented by the quantitative results of Tani, et al.[19] They give information on velocity profiles downstream of cylindrical roughness elements that supports the existence of the two sets of downstream vortices determined visually. These tests were made for zero pressure gradient flow over a flat plate with freestream speed from 3–15 m/sec; two different wind tunnels were used with substantially different turbulence levels, viz., 0.05% and 0.2%. In addition to the results reviewed here, they investigated the downstream development of controlled 2-D disturbances induced by a vibrating ribbon placed downstream of the roughness element.

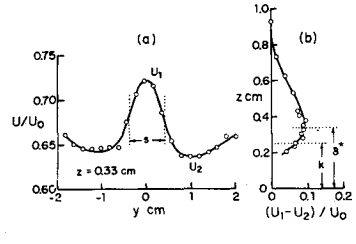

Fig. 7 a) Spanwise distribution of mean velocity in the x direction. b) Distribution across the boundary layer of the velocity difference. Parameters the same as for Fig. 6, except x-$x_k = 61$ cm. From Ref. 19.

At $X = 10$ the velocity distributions, reproduced here in Fig. 6, were indicative of two sets of vortices, the horseshoe and trailing vortices. For two values of z, the distribution of flow direction in the xy plane is also given; a maximum value of the cross-flow direction of 3° is measured. These show that an S-shaped cross-flow profile must exist at this station. At $X = 244$ the results shown in Fig. 7 were obtained. The double peak in the u distribution has now disappeared which suggests decay of the spiral-trailing vortex but not of the horseshoe vortex; however no cross flow could be detected. Although no idea of the degree of unsteadiness is given, it turns out that conditions for Figs. 6 and 7 are almost the same as those for Fig. 3, $U = 5.3$ m/sec; this picture shows only a very slight waviness in the vortex at these downstream distances. Figure 7 presents the notation used for the maximum and minimum of u, u_1 and u_2 respectively, and for s which is defined by the distance between the two points where $u = (u_1+u_2)/2$ and is taken to be a measure of the spacing of the horseshoe vortex trails. Note that the decay of u_1-u_2 with z is consistent with the boundary-layer nature of the flow.

The effect of the horseshoe vortex is remarkably persistent as shown in Fig. 8 (also from Ref. 19). The spacing appears to scale with k and to change little; the maximum velocity difference is essentially constant after 100 roughness heights. It is further noted that the velocity distribution across the boundary layer at the peaks and valleys agrees with the Blasius profile, to within experimental accuracy.

Thus we have a fairly complete picture of the perturbation caused by a 3-D protuberance in a low-speed laminar boundary layer. This can offer guidance in other flow regimes since, as mentioned in the introduction at least some elements are common to all regimes.

b) *Turbulent flow:* When an isolated 2-D protuberance is inserted in a turbulent boundary layer the same general phenomena occur as for the laminar case: separation upstream and downstream, reattachment, and recovery to an equilibrium profile. Some details are given in Mueller, et al.[21] Tani has reviewed the latter and also some other examples of sudden perturbations to a turbulent boundary layer. He concludes that the recovery to equilibrium is almost instantaneous near the wall but rather slow in the outer part of the boundary layer initiated by reattachment. The measurements of Mueller show that downstream of reattachment "the sequence of profile shapes appears to be simply traversed in a reverse sense as compared to a boundary layer developing toward separation." The non-

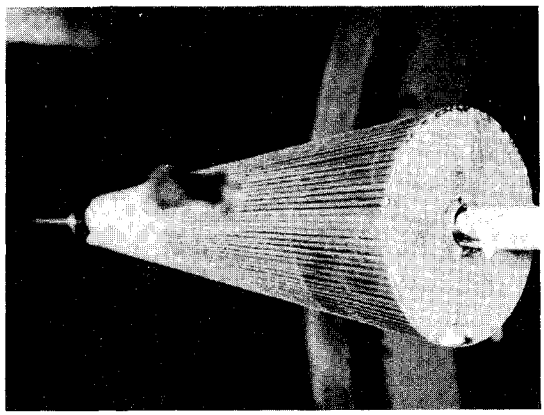

Fig. 9 Persistence of downstream vortices shown by the striations in a surface oil film. Transition is induced by a row of 47 cubes placed at 21% of the length of a 10° cone. $k = 0.01$ in., $M = 4$. Courtesy L. Kayser, BRL.

local effects of a protuberance on the bounday layer appears as a "diffusion-like effect" (see the discussion of Tani's paper by Kline, p. 527 of Ref. 22). Many investigators have examined the perturbations to a turbulent boundary layer caused by distributed roughness elements; a review of this work will not be attempted here.

Data are very limited for a 3-D protuberance in a turbulent boundary layer. Prandtl[23] presents one picture, from the work of A. Hinderks, of the surface streamline pattern caused by a plate mounted on the bottom of a water channel. The front part of the horseshoe vortex and evidence of two symmetrically located spirals behind the plate are clearly seen. In a study of cavitation inception on 3-D roughness elements Benson[24] shows evidence of the horseshoe vortex for a hemispherical protuberance; cavitation in the core of the vortex makes it visible. Morkovin[20] also mentions the existence of one such vortex in a turbulent boundary layer. In a review article McCormick[25] shows a flow pattern (due to Halitsky) "around a simple cubical building, and the disposition of pollutants emitted at three different locations above it as determined in a wind tunnel." The flow model seems much more appropriate to 2-D flow, however. There is obviously a need for additional work in this area.

2. High-Speed Flow

a) *Laminar:* For transonic and low supersonic Mach numbers the interest in protuberances is motivated mainly by their contribution to the total drag or their effect on the location of boundary-layer transition. For most vehicles the protuberances are immersed in a turbulent boundary layer. The contribution to drag is an important consideration but is not a topic of this review; much work has been done on this (see Ref. 26 and references therein). For $M > 3$, where M is freestream Mach number, consideration of the increased heating (hot spots) caused by small protuberances or depressions becomes important, even if laminar flow is maintained.[5,27]

There is a wealth of data on transition caused by 2-D and 3-D roughness elements but there are apparently many pitfalls in interpreting and using the data.[5] In general it is found that, compared to the low-speed case, k/δ_k must be closer to unity for transition to be affected by a roughness element at supersonic speeds, and $k/\delta_k > 1$ for the hypersonic case. As M increases it becomes more difficult to trip the boundary layer at all; Holloway and Sterrett[28] show evidence that, under some conditions, transition can be delayed for $M \gtrsim 3.7$ and $k/\delta_k < 1$. For 3-D roughness elements, flowfield distortions, indicative of the horseshoe vortices, persist far downstream into the turbulent boundary layer. A striking illustration of this phenomenon is shown in Fig. 9, from the work of L. Kayser of BRL. The boundary layer on a 10° half-angle cone with $M = 4.0$ was tripped by a row of cubes, $k = 0.01$ in. with spacing 0.046 in., placed at 21% of the cone length. An oil mixture was spread on the surface (not specifically for studying protuberance effects). The model was photographed after the test. The striations are not visible in the transition region but appear in the turbulent region and persist to the base of the cone. There appear to be two striae for each cube. Sometimes these flowfield distortions are not readily apparent on the surface but are detected off the surface in the boundary layer,[29,30] possibly due to the spacing of the roughness elements. This persistence into the turbulent region has also been found in heat-transfer tests.[27]

Experiments on 2-D protuberances in laminar flow have been performed at hypersonic speeds mainly to document the large, local effect they have on heat transfer. For example, single protuberances (and depressions) of various shapes were investigated by Bertram and Wiggs[31]; multiple, sine-waves shapes were treated by Bertram, et al.[32] and Arrington.[33] Surface visualization by the oil-flow method was used to study two-dimensionality and separation of the flow. In Ref. 31 results are given for $0.2 \leqq k/\delta_k^* \leqq 10$, $M = 6.8$ and 9.6, flat plates with sharp and blunt leading edges, and angles of attack up to 20°. The local Mach number at x_k, M_k, varied from 1.7 to 10.4. The flow separated upstream (as much as $8k$), reattached on the protuberance, separated again and then reattached downstream. The changes in pressure were relatively mild but dramatic changes in heat transfer took place of the type that have been found in many studies of separating and reattaching flows on larger scales. Relative to the undisturbed flow the heat transfer decreased in separated flow and increased sharply at reattachment. Taking account of the corrections to Ref. 31 noted in Ref. 32, the maximum heat transfer was as much as 25 times the undisturbed value; although there is considerable scatter the ratio can be correlated by

$$h_{\max}/h_{fp} = 1 + (1/36)[M_k k/\delta_k^*]^{1.9}$$

where h is the film heat-transfer coefficient and the subscript fp refers to the smooth, flat-plate value. For the larger unit Reynolds numbers (approximately 0.4×10^6/in.) streamwise vortices were detected in the oil-flow patterns. These patterns were found in pairs across the span and were correlated with the appearance of transition or turbulence in the separated flow. Some examples of these are shown in Ref. 33. For the multiple sine-wave surface distortion, when the flow clearly remained laminar,[33] the oscillations in heat transfer were approximately in phase with the surface wave. When the effect of orientation of single or multiple distortions was considered,[34] no significant change in maximum heat transfer was found for angles of sweepback up to 70°.

Most of the experiments on 3-D protuberances in laminar flow were done in connection with transition studies. With few exceptions only surface flow visualization and heat-transfer measurements have been used to probe the flowfield. In the upstream separated flow the front part of the horseshoe vortex system has been detected[35] and downstream streaks appear indicating the persistence of at least one of the horseshoe vortices. In all cases a row of roughness elements was used, and there is no doubt interaction between the downstream portions of the horseshoe vortices from the individual roughness elements. Usually only two streaks are seen downstream of each roughness element, although occasionally, e.g., van Driest and McCauley,[36] additional streaks are found. If k is small enough a single streak may be observed, van Driest et al.[37]; again it can be conjectured that the two streaks cannot be resolved in this case. Actually Korkegi[38] seems to have been the first to report the presence of the twin streaks caused by either a roughness element or a small area of air injection into a flat-plate flow.

The most obvious difference in the disturbed flowfields between the low-speed and high-speed cases is that the latter will have a system of shock waves. A separation shock and a

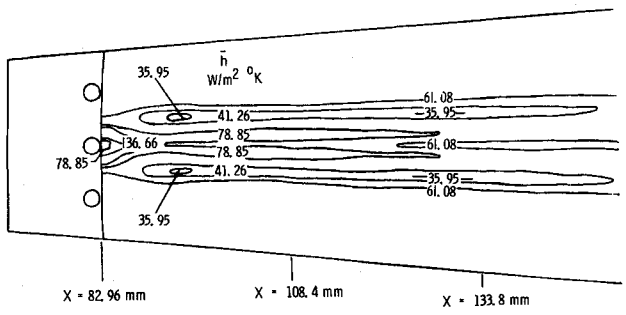

Fig. 10 Heat-transfer distribution behind a row of spherical roughness elements. Laminar flow over a blunted 5° cone. $k/\delta_k^* = 3.29$, $M = 8$. From Ref. 27.

bow shock will merge into one to give a λ shock formation; there may be more than one triple point as has been found for large protuberances in a turbulent boundary layer[39] or other examples of interacting shocks.[40] A "reattachment" shock will also occur downstream. An example of these, but for a turbulent boundary layer, will be shown later. A quantitative assessment of this shock system on the flowfield has not been attempted.

An extensive surface flow visualization study was made by Whitehead.[35] Results are shown for spheres, cylinders, triangular prisms, and pinheads although other shapes were tested. The oil patterns led him to conclude that four vortices, rotating in opposite directions, exist upstream of the protuberances. Conditions for the tests were: $M_k = 4.7$ and 5.5, R_{x_k} varied from 1.95×10^5 to 13.10×10^5, and $1 \leqq k/\delta_k \leqq 4$ where δ_k was determined from measured velocity profiles; the elements were mounted on wedges. The lateral spacing l of the elements was varied and for $l \geqq 8k$ the upstream separation regions of adjacent elements did not interact. For this latter condition and $k/\delta_k = 2$, the upstream separation distance from the center of the element was $6k$ for the cylinder but $3k$ for the other shapes. No information on the downstream flowfield is given; the elements were located approximately $3\delta_k$ from the trailing edge so that some upstream base influence might have occurred.

Downstream effects are shown in Ref. 27 using heat sensitive paint to measure heat transfer. One such result is given in Fig. 10 which shows not only the persistence of the downstream effect but also the rapid spatial variation in heat transfer. Transition occurred at $x = 220$ mm. The maximum heat transfer, which is four times the minimum, occurs near the neck of the horseshoe vortex. Enlargements of the paint pattern pictures shown in Ref. 35 show remarkable similarities to the smoke pictures in Fig. 4. In a related vein, Whitfield and Iannuzzi[41] show one result for which, although transition did not occur, the heat transfer on a cone at $M = 15$ was about half way between the expected laminar and turbulent results at $X = 175$ behind a spherical roughness element.

Flowfield surveys off the surface present difficulties; one such attempt is mentioned in Ref. 29. "Hot wire surveys of the near flowfield of spherical roughness elements were obtained, but because of the complexity of the flow and the long wire lengths relative to the roughness element size, little useful information was derived." Actually some of the scales of the flowfield are significantly smaller than k.

Finally it is of interest to review briefly the work on streamwise vortices in laminar reattaching flows (see Ginoux[42] and the references cited therein). These vortices represent 3-D perturbations in a 2-D boundary layer and have surprisingly large effects; the maximum effect occurs during the transition process. "The intensity of the flow perturbations was roughly in proportion to the size of very small irregularities of manufacture of the leading edge of the models, although their spacing was not influenced by the size or distribution of these irregularities." In the cited reference a more controlled test was made by placing small strips of scotch tape near the leading edge. One or two rows of counter-rotating streamwise vortices were found. Surface heat-transfer measurements of high spatial resolution (less than 1 mm) showed rapid variations in the spanwise direction; the peaks in heat transfer were considerably higher ($\sim 50\%$) than that obtained with turbulent reattachment. Thus we have another example of large and persistent effects caused by small 3-D perturbations in a 2-D laminar boundary layer.

b) *Turbulent:* Many investigators have studied either separating or reattaching flows for, hopefully, 2-D conditions. Since the general flow pattern for turbulent flow over protuberances is expected to be the same as for the laminar case, viz., two regions involving separation and attachment, the elements of the flowfield can be pieced together. Two major questions that arise concern departure from two-dimensionality and unsteadiness of the flow. The former was mentioned in Sec. 2a when discussing the results of Refs. 31–33. The high degree of unsteadiness at the separation point was documented by Kistler.[43]

The experiments in high-speed turbulent boundary layers have dealt mainly with large 3-D protuberances.[2] Since some of the features of the upstream, disturbed flow are qualitatively the same for small or large k some results for large k will be mentioned. Most information is given for cylindrical protuberances or slabs with cylindrical leading edges. The separation distance, measured from the leading edge of the cylinder, decreases linearly with diameter.[39] For $k > \delta_k$ the separation distance depends weakly on k but as $k \to \delta_k$ it decreases sharply.[39,44] The dependence on M and Re_{x_k} is weak.[44] For large k there is evidence of several vortices in the upstream separation region,[39,45] but for $k/\delta_k < 1$ the evidence seems to indicate one large-scale vortex and a small-scale vortex located very close to the cylinder base, see the discussion below. This small-scale vortex is indicated by an attachment line in the surface flow visualization and is also found for large k.[45,46] Winkelmann[45] related the location of this attachment line to the maximum heating rate on the surface. Because the shear stress is also large in this region this attachment line is often not detected in surface flow visualization. In particular it has not been reported in the visual studies of high-speed laminar or low-speed laminar and turbulent flows. In Ref. 46, for large k, it is conjectured that this is an attachment line of a stream surface that leaps over the main vortex system and impinges on the surface. Another possibility, partially supported by the results of Ref. 47, is that it comes from the flow separating off the protuberance.

Korkegi[2] summarizes the available results for pressure and heat-transfer distributions, most of which are for large k. Some additional, rather limited data is given by Halprin.[48] The matter of unsteadiness in the flow has apparently not been considered. That the flow is unsteady, at least near the protuberance, is evident from shadowgraphs taken with a short duration (1μsec) light source. One of these is shown in Fig. 11, showing the side view of a rectangular prism mounted on the wall of one of the BRL supersonic wind tunnels. The unit Reynolds number

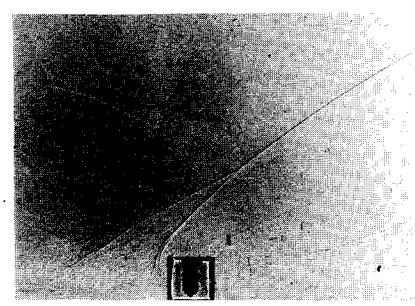

Fig. 11 Side view shadowgraph of a rectangular prism in a turbulent boundary layer, k = length = 0.80 in., width = 1 in., $\delta_k = 1$ in., $M = 2.50$, unit Reynolds number 0.24×10^6/in.

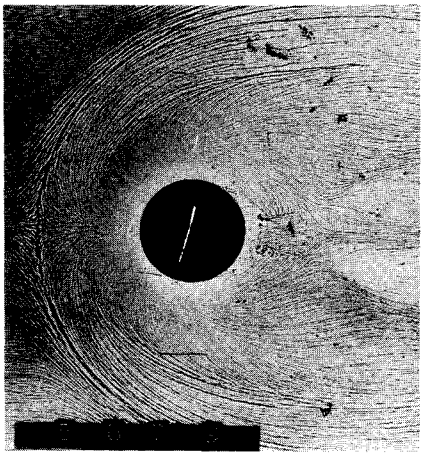

Fig. 12 Plan view shadowgraph of a cylinder, diameter 1.50 in., in a turbulent boundary layer. Oil droplets are placed on the window. $k = 0.80$ in., $\delta_k = 1$ in., $M = 2.50$, unit Reynolds number 0.24×10^6/in.

is 0.24×10^6/in., $M = 2.50$, $k/\delta_k = 0.8$. The bow wave near the protuberance appears at different positions in pictures taken at different times; this will be seen in the plan view shadowgraphs discussed next.

Some examples of surface flow visualization for small protuberances will now be presented. These were taken in the facility mentioned and for conditions given in the preceding paragraph. The technique, described in Ref. 46, combines the oil-flow method and an optical system to visualize the disturbed flow when a protuberance is mounted on the window of the wind tunnel. The transparent oil is either placed on the window before the test is started or a small amount is aspirated into the boundary layer during the test, through a static pressure tap located upstream of the window frame. Shadowgraph and schlieren pictures are taken before, during, and after the test. When oil droplets are sprayed at random on the window over the disturbed flow region and a plan view shadowgraph is taken during the flow, the result is a pattern shown in Fig. 12. When the oil is sprayed only in the region upstream of separation and several rows of oil dots are placed downstream

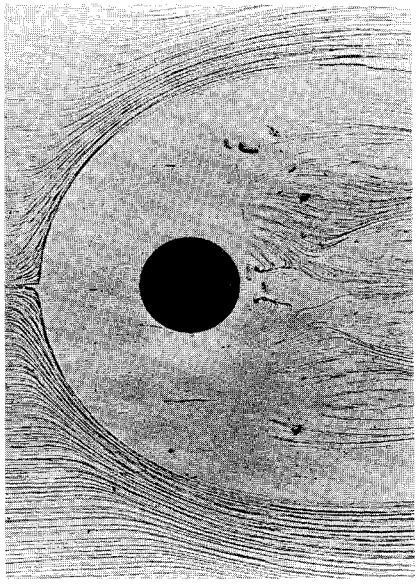

Fig. 13 Plan view shadowgraph. Oil droplets placed upstream of separation and several rows of oil dots placed downstream of the cylinder. Conditions same as for Fig. 12.

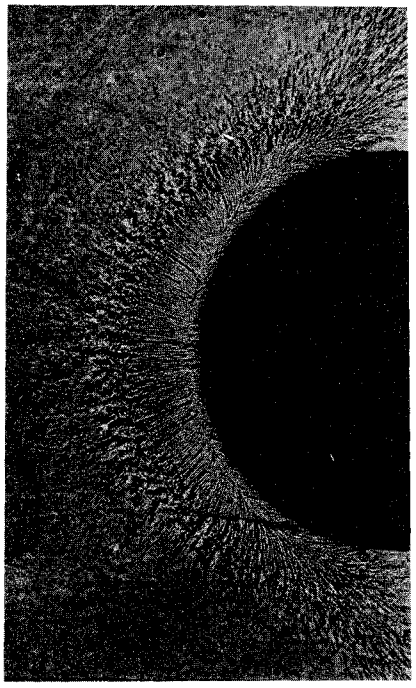

Fig. 14 Enlargement of plan view shadowgraph showing upstream attachment line. Oil aspirated into the boundary layer. Conditions same as for Fig. 12.

of the cylinder the result shown in Fig. 13 is obtained. The latter delineates the main separation more clearly than the former.

Since shock shadows appear only for light rays at grazing incidence to the shock surface, only a portion of the bow wave appears in these plan view shadowgraphs (refer to Fig. 11). The position and form of these shock shadows are noticeably different in Figs. 12 and 13. Although these were taken in different tests the same variability is found in a given test when the pictures are taken at intervals of several seconds. (The shock shadows are easily distinguished from window defects since the latter are fixed.) This illustrates the unsteady aspect of the flowfields. The surface streamlines, however, remain fixed after the initial development time.

Although oil droplets were placed immediately upstream of the cylinder, in Fig. 12 the pattern is completely erased by the flow. The flow pattern in this region is obtained when oil is aspirated into the flow, as shown in Fig. 14. This enlarged view of the region upstream of the cylinder clearly shows the attachment line discussed above; the distance from the cylinder surface is 0.030 times the cylinder diameter. (For the same conditions except $k/\delta_k = 4$, this ratio is 0.043.) Therefore in addition to the large-scale vortex there must be at least one other, counter-rotating, vortex of scale size much smaller than the diameter. A clearly defined secondary separation line is shown in the surface flow visualization work by Winkelmann[45] for a fin protuberance with a cylindrical leading edge and $k/\delta_k = 2.3$; between this and the primary separation line a nodal point of attachment is found. He concludes that there are four counter-rotating vortices in the upstream separated flow.

An interesting feature of Figs. 12 and 13 is the surface streamline pattern in the near wake. An oil accumulation line departs from the cylinder at about 120° from the forward generator; this is probably the intersection with the wall of the lateral vortex sheet mentioned by Morkovin.[20] This line meets another accumulation line along which the flow is upstream. They join, together with streamlines closer to the axis, to form an accumulation point. The spiral motion near that point would appear to be the surface trace of the spiral vortex shown in the sketch (Fig. 2) and the smoke picture (Fig. 4). The number of

streamlines, entering the neck of the near wake and then proceeding upstream, is hard to interpret unless it is postulated that flow impinges on the surface along a line which ends in the "saddle point" type of stagnation point. Although the evidence is sketchy from these surface streamline patterns, it would appear that this entrance into the near wake and the apparent spiral vortex illustrate Morkovin's base flow-through module for high-speed turbulent flow over a protuberance.

Extensive investigation by visual means has not been made for the downstream flow. Pressure surveys are given in Ref. 49 but it is difficult to interpret these for the highly 3-D flowfield. The persistence of the longitudinal vortices found in the other cases discussed previously is possible, as shown in Fig. 9. However in this case, and others referred to in the discussion of Fig. 9, the protuberances were in an initially laminar boundary layer and the flow perturbation is influenced by the transition process.

In addition to the simple geometrical shapes just discussed, results are reported in Refs. 49–52 for shapes representative of protuberances on vehicles. The effect of a gap between the protuberance and surface has also been investigated.[53] Rectangular shapes with large aspect ratio were tested by Burbank et al.[54] Even for an aspect ratio of 24 there is a significant departure from two-dimensional flow. Surface flow visualization for a case with aspect ratio 12 and $k/\delta_k = 0.67$ shows spiral vortices at the ends and a "loop" vortex with 3-D structure in the near wake.

III. Review of Analytical Work

Some analytical work for the 2-D problem has been done for the case of a low Reynolds number shear flow past a protuberance. Dean[55] considered a one-parameter family of shapes for which the boundary could be represented as a circle (after a conformal transformation) by a rational function of the independent variable in the transformed plane. These shapes were symmetrical about a line normal to the undisturbed shear flow direction. Unless the parameter is unity, the boundary shape is smooth and it is found that, if a critical velocity is exceeded, a closed vortex is formed on the downstream side of the protuberance. If the parameter is unity, the boundary has a sharp edge and the closed vortex is formed for all velocities. Similar results were found for unsymmetrical boundaries.[56] For a linear shear flow, Gertsenshstein[57] considered a cylindrical protuberance of semicircular cross section placed on a flat plate. The linearized Navier-Stokes equations were solved by the Bubnov-Galerkin method using ten terms in the series. The only discussion of the results is a qualitative one with regard to the stability of the resultant flow. Schubert[58] gives a brief discussion of low Reynolds number shear flow over circular projections and depressions in a flat plate; actually, details are given only for the latter. In these papers no attempt is made to relate the results to a boundary-layer flow by a consistent approximation scheme.

Such an attempt was made by Hunt[59] who considered a linearized perturbation of the Navier-Stokes equations for the flow near the surface assuming $k \ll \delta_k$. With the aid of some additional assumptions he is able to get a solution for the perturbation velocity. He concludes that a certain integral, related to the moment exerted on the protuberance, is a constant along the wake and that the perturbation decays as x^{-1} compared to $x^{-1/2}$ for the wake of a body in uniform flow. No comparison with experimental results is given since the available data are not detailed enough; perhaps a comparison with the data of Ref. 15 will be feasible.

Several examples of 2-D perturbation solutions have been worked out, strictly within the framework of boundary-layer theory. Libby and Fox[60] considered perturbations about the compressible flow Blasius solution of the momentum equation. Fox and Libby[61] presented a similar analysis for the energy equation. Chen and Libby[62] studied perturbations of the momentum equation about the Falkner-Skan solution and Chen[63] did the analogous problem for perturbations of the energy equation. All of these require the solution of eigenvalue problems and give results for a linearized analysis of small deviations from the basic flow. Serrin[64] has proved, without linearization, for a favorable pressure gradient of the power law type and some mild restrictions on an initial profile, that the velocity will approach asymptotically the Falkner-Skan solution. For this incompressible flow the rate of convergence was also estimated. The results of Chen and Libby[62] are in accord with Serrin's results but they also conclude that for the "lower branch solutions," corresponding to reverse flow, the perturbed flows are spatially unstable. Much of the detailed work can be carried out analytically for perturbations of laminar flows. Using finite difference methods on the turbulent boundary-layer equations and a rate equation for the turbulent viscosity, Nee and Kovasznay[65] calculated the response to perturbations of an initial profile. When the disturbance was distributed over the entire layer, the inner portion showed a higher damping rate than the outer region. Results were also presented for the decay of a more concentrated disturbance.

The analytical work that most closely resembles the 3-D perturbed flow patterns found experimentally is that of Hawthorne and Martin.[66] Assuming inviscid flow, the effects of shear and density gradient are found for a hemispherical protuberance on a flat surface. A linear perturbation about the potential flow is considered. The perturbation becomes infinite at a stagnation point, however, so that the assumptions on which the analysis is based are not valid in, e.g., the region immediately upstream of the protuberance. Nevertheless streamwise vortices are found which persist for $x \to \infty$. As noted in Ref. 66, the actual flow pattern would be considerably modified by induced velocities and viscous effects but at least there is qualitative agreement with the observed horseshoe vortex.

An attempt to analyze the downstream effects of initially induced streamwise vorticity has been made by Sedney,[67] in the spirit discussed in the Introduction. If no spanwise variations in cross flow exist then several classes of exact solution are constructed in terms of the eigenfunctions derived in Refs. 59 and 61. These show that the surface vorticity decreases about twice as fast for an S-shaped initial profile as compared to a C-shaped profile. Because of the restriction of no spanwise variation, comparison with experimental results on protuberance flowfields is not possible. Even with this restriction, rather slow decay of streamwise vorticity is shown. When a linearized perturbation method is used to handle spanwise variations, a kind of spatial instability is found.

The 3-D perturbations found in experimental results are so complex in the neighborhood of the protuberance that it is unlikely that an analysis can be developed that is capable of describing that part of the flowfield. There is hope that progress can be made analyzing the downstream flowfield.

IV. Conclusions and Summary

From the review of representative data on boundary-layer flows over small protuberances, the following conclusions can be drawn. For the 2-D case the over-all flow perturbations are about as expected. The general features can be understood from the large body of information on separating and reattaching flows. Since unexpected 3-D effects occur and unsteadiness is not sufficiently documented, caution is needed when interpreting the data. More detailed measurements on the flowfield are required in order to evaluate analytical predictions for the downstream perturbations. No rational approximation schemes have been proposed to analyze the flow in the neighborhood of the protuberance.

For the 3-D case the flow perturbations are complex but contain vortex patterns that are common to a wide range of conditions. These are the vortex system in the upstream separated flow, the spiral vortices in the near wake, and the horseshoe vortex system. A more tentative conclusion is that the

base region, with flow in, near the neck and out, by means of the spiral vortices, is also a common feature. Qualitatively these elements are similar enough that results from, say, low-speed laminar flow can be used for guidance in interpreting those for high-speed turbulent flow. The quantitative aspects of these elements, e.g., the number of vortices in the upstream separated flow and their subsequent behavior, vary with the dimensionless parameters and the type of flow. To obtain the details of this variation experimentally would require an extensive series of tests. Guidance from theory or numerical calculations would be beneficial but is presently not available.

For high-speed flow, even if transition does not occur, there are local regions of high heating rates near a protuberance and rates significantly higher than those for laminar flow far downstream. The remarkable persistence of downstream effects is the most distinguishing feature of 3-D perturbations compared to the 2-D case.

Progress has been made in constructing physical models of the flow perturbations caused by small protuberances. This can be utilized in formulating mathematical models which, in turn, can help guide experimental work. The returns from such studies will be applicable to a wide class of technologically important flows.

References

[1] Sedney, R., "A Review of the Effects of Steady, Three-Dimensional Perturbations in a Laminar Boundary Layer," TR 71–24, July 1969, Research Institute for Advanced Study, Baltimore, Md.

[2] Korkegi, R. H., "Survey of Viscous Interaction Associated With High Mach Number Flight," *AIAA Journal*, Vol. 9, No. 5, May 1971, pp. 771–784.

[3] Tani, I., "Review of Some Experimental Results on Boundary-Layer Transition," *The Physics of Fluids*, Vol. 10, No. 9, Sept. 1967 (Supplement), pp. 511–516.

[4] Tani, I., "Boundary-Layer Transition," *Annual Review of Fluid Mechanics*, Vol. 1, Annual Reviews, Palo Alto, Calif., 1969, pp. 169–196.

[5] Morkovin, M. V., "Critical Evaluation of Transition from Laminar to Turbulent Shear Layers With Emphasis on Hypersonically Traveling Bodies," TR-68-149, March 1969, Air Force Flight Dynamics Lab., Wright-Patterson Air Force Base, Ohio; also available as TR-68-13c, Dec. 1968, Research Institute for Advanced Study, Baltimore, Md.

[6] Henderson, A. Jr., "Hypersonic Viscous Flows," *Modern Developments in Gas Dynamics*, edited by W. H. T. Loh, Plenum Press, New York, 1969, pp. 83–129.

[7] Lin, C. C. and Benney, D. J., "On The Instability of Shear Flows," *Proceedings of Symposia in Applied Mathematics, Hydrodynamic Instability*, American Mathematical Society, Providence, R.I., Vol. 13, 1962, pp. 1–24.

[8] Stuart, J. T., "Hydrodynamic Stability," *Applied Mechanics Review*, Vol. 18, No. 7, July 1965, pp. 523–531.

[9] Leibovich, S. and Koh, B., "Secondary Flow Induced by Weakly-Sheared Cross Flow Past a Slender Body," AIAA Paper 68–715, Los Angeles, Calif., 1968.

[10] Lighthill, M. J., "The Fundamental Solution for Small Steady Three-Dimensional Disturbances To A Two-Dimensional Parallel Shear Flow," *Journal of Fluid Mechanics*, Vol. 3, Pt. 2, 1957, pp. 113–144.

[11] Sedney, R., "Some Aspects of Three-Dimensional Boundary Layer Flows," *Quarterly of Applied Mathematics*, Vol. 15, No. 2, July 1957, pp. 114–122.

[12] Squire, L. C., "The Three-Dimensional Boundary-Layer Equations and Some Power Series Solutions," R. & M. 3006, 1957, Aeronautical Research Council, England.

[13] Rosenhead, L., ed., *Laminar Boundary Layers*, Clarendon, Oxford, 1963, p. 457.

[14] Tani, I. and Sato, H., "Boundary-Layer Transition by Roughness Element," *Journal of the Physical Society of Japan*, Vol. 11, No. 12, Dec. 1956, pp. 1284–1291.

[15] Klebanoff, P. S. and Tidstrom, K. D., "Mechanism By Which a Two-Dimensional Roughness Element Induces Boundary Layer Transition," *The Physics of Fluids*, Vol. 15, No. 7, July 1972, pp. 1173–1188.

[16] Gregory, N. and Walker, W. S., "The Effect of Transition of Isolated Surface Excrescences in the Boundary Layer," R. & M. 2779, Pt I, 1955, Aeronautical Research Council, England.

[17] Thwaites, B., ed., *Incompressible Aerodynamics*, Oxford University Press, England, 1960, p. 554.

[18] Mochizuki, M., "Smoke Observation on Boundary Layer Transition Caused by a Spherical Roughness Element," *Journal of Physical Society of Japan*, Vol. 16, No. 5, May 1961, pp. 995–1008.

[19] Tani, I., Komoda, H., Komatsu, Y., and Iuchi, M., "Boundary-Layer Transition by Isolated Roughness," Rept. 375, Nov. 1962, Aeronautics Research Inst., Univ. of Tokyo, Tokyo, Japan, pp. 129–142.

[20] Morkovin, M. V., "An Approach to Flow Engineering Via Functional Flow Modules," Beiträge zur Strömungsmechanik, insbesondere zur Grenzschichttheorie Teil 2, Deutsche Luft- und Raumfahrt Forschungsbericht 72-27, 1972, pp. 270–301.

[21] Mueller, T. J., Korst, H. H., and Chow, W. L., "On The Separation, Reattachment, and Redevelopment of Incompressible Turbulent Shear Flow," *Journal of Basic Engineering*, Vol. 86, Series D, No. 2, June 1964, pp. 221–226.

[22] Tani, I., "Review of Some Experimental Results on the Response of a Turbulent Boundary Layer to Sudden Perturbations," *Proceedings on the Computation of Turbulent Boundary Layers—1968 AFOSR-IFP-Stanford Conference*, Vol. I, pp. 483–494.

[23] Prandtl, L., *Essentials of Fluid Dynamics*, Hafner, New York, 1952, p. 147.

[24] Benson, B. W., "Cavitation Inception on Three-Dimensional Roughness Elements," Rept. 2104, May 1966, David Taylor Model Basin, Naval Ship Research and Development Center, Washington, D.C.

[25] McCormick, R. A., "Air Pollution in the Locality of Buildings," *Philosophical Transactions of the Royal Society, Series A*, Vol. 269, 1971, pp. 515–526.

[26] Czarnecki, K. R. and Monta, W. J., "Roughness Drag Due to Two-Dimensional Fabrication-Type Surface Roughness on an Ogive Cylinder from Force Tests at Transonic Speeds," TN D–5004, Jan. 1969, NASA.

[27] Stainback, P. C., "Effect of Unit Reynolds Number, Nose Bluntness, Angle of Attack, and Roughness on Transition on a 5° Half-angle Cone at Mach 8," TN D–4961, 1969, NASA; also AIAA Paper 67-132, New York, 1967.

[28] Holloway, P. F. and Sterrett, J. R., "Effect of Controlled Surface Roughness on Boundary-Layer Transition and Heat Transfer at Mach Number of 4.8 and 6.0," TN D–2054, April 1964, NASA.

[29] Morrisette, E. L., Stone, D. R., and Cary, A. M., Jr., "Downstream Effects of Boundary-Layer Trips in Hypersonic Flows," *Compressible Turbulent Boundary Layers*, NASA SP–216, 1969, pp. 437–453.

[30] Sterrett, J. R., Morrisette, E. L., Whitehead, A. H., Jr., and Hicks, R. M., "Transition Fixing for Hypersonic Flow," TN D–4129, Oct. 1967, NASA.

[31] Bertram, M. H. and Wiggs, M. M., "Effect of Surface Distortions on the Heat Transfer to a Wing at Hypersonic Speeds," *AIAA Journal*, Vol. 1, No. 6, June 1963, pp. 1313–1319.

[32] Bertram, M. H., Weinstein, L. M., Cary, A. M., Jr., and Arrington, J. P., "Heat Transfer to Wavy Wall in Hypersonic Flow," *AIAA Journal*, Vol. 5, No. 10, Oct. 1967, pp. 1760–1767; also erratum: this article, *AIAA Journal*, Vol. 6, No. 6, June 1968, p. 1216.

[33] Arrington, J. P., "Heat Transfer and Pressure Distributions Due to Sinusoidal Distortions on a Flat Plate at Mach 20 in Helium," TN D–4907, Nov. 1968, NASA.

[34] Jaeck, C. L., "Analysis of Pressure and Heat Transfer Tests on Surface Roughness Elements With Laminar and Turbulent Boundary Layers," CR–537, 1966, NASA.

[35] Whitehead, A. H., Jr., "Flow-field and Drag Characteristics of Several Boundary-Layer Tripping Elements in Hypersonic Flow," TN D–5454, Oct. 1969, NASA.

[36] van Driest, E. R. and McCauley, W. D., "The Effect of Controlled Three-Dimensional Roughness on Boundary-Layer Transitions at Supersonic Speeds," *Journal of the Aerospace Sciences*, Vol. 27, No. 4, April 1960, pp. 261–271, 303.

[37] van Driest, E. R., Blumer, C. B., and Wells, C. S., Jr., "Boundary-Layer Transition on Blunt Bodies—Effect of Roughness," *AIAA Journal*, Vol. 5, No. 10, Oct. 1967, pp. 1913–1915.

[38] Korkegi, R. H., "Transition Studies and Skin-Friction Measurements on an Insulated Flat Plate at a Mach Number of 5.8," *Journal of the Aeronautical Sciences*, Vol. 23, No. 2, Feb. 1956, pp. 97–107.

[39] Voitenko, D. M., Zubkov, A. I., and Panov, Yu. A., "Supersonic Gas Flow Past a Cylindrical Obstacle on a Plate," *Mekhanika Zhidkosti i Gaza*, Vol. 1, No. 1, Jan.–Feb. 1966, pp. 121–125; also *Journal of Fluid Dynamics*, Vol. 1, 1966, pp. 84–88 (Faraday Press Translation).

[40] Edney, B. E., "Effects of Shock Impingement on the Heat Transfer Around Blunt Bodies," *AIAA Journal*, Vol. 6, No. 1, Jan. 1968, pp. 15–21.

[41] Whitfield, J. D. and Iannuzzi, F. A., "Experiments on Roughness Effects on Cone Boundary-Layer Transition Up to Mach 16," *AIAA Journal*, Vol. 7, No. 3, March 1969, pp. 465–470.

[42] Ginoux, J. J., "Streamwise Vortices in Laminar Flow," *Proceedings of a Specialist Meeting, Recent Developments in Boundary Layer Research, Pt. I*, AGARDograph 97, Italy, May 10–14, 1965, pp. 395–422.

[43] Kistler, A. L., "Fluctuating Wall Pressure Under a Separated Flow," *Journal of the Acoustical Society of America*, Vol. 36, No. 3, March 1964, pp. 543–550.

[44] Westkaemper, J. C., "Turbulent Boundary-Layer Separation Ahead of Cylinders," *AIAA Journal*, Vol. 6, No. 7, July 1968, pp. 1352–1355.

[45] Winkelmann, A. E., "Flow Visualization Studies of a Fin Protuberance Partially Immersed in a Turbulent Boundary Layer at Mach 5," NOLTR 70–93, May 1970, Naval Ordnance Lab., White Oak, Md.

[46] Sedney, R., "Visualization of Boundary Layer Flow Patterns Around Protuberances Using an Optical-Surface Indicator Technique," *The Physics of Fluids*, Vol. 15, No. 12, Dec. 1972, pp. 2439–2441.

[47] Voitenko, D. M., Zubkov, A. I., and Panov, Yu. A., "Existence of Supersonic Zones in Three-Dimensional Separation," *Mekhanika Zhidkosti i Gaza*, Vol. 2, No. 1, 1967, pp. 20–24; also *Journal of Fluid Dynamics*, Vol. 2, 1967, pp. 13–16 (Faraday Press Translation).

[48] Halprin, R. W., "Step Induced Boundary-Layer Separation Phenomena," *AIAA Journal*, Vol. 3, No. 2, Feb. 1965, pp. 357–359.

[49] Couch, L. M., "Flow-Field Measurements Downstream of Two Protuberances on a Flat Plate Submerged in a Turbulent Boundary Layer at Mach 3.49 and 4.44," TN D–5297, July 1969, NASA.

[50] Stallings, R. L., Jr. and Collins, I. K., "Heat-Transfer Measurements on a Flat Plate and Attached Protuberances in a Turbulent Boundary Layer at Mach Numbers of 2.65, 3.51, and 4.44," TN D–2428, Sept. 1964, NASA.

[51] Price, E. A., Jr. and Stallings, R. L., Jr., "Investigation of Turbulent Separated Flows in the Vicinity of Fin-Type Protuberances at Supersonic Mach Numbers," TN D–3804, Feb. 1967, NASA.

[52] Price, E. A., Howard, P. W., and Stallings, R. L., Jr., "Heat-Transfer Measurements on a Flat Plate and Attached Fins at Mach Numbers of 3.51 and 4.44," TN D–2340, June 1964, NASA.

[53] Winkelmann, A. E., "Experimental Investigations of a Fin Protuberance Partially Immersed in a Turbulent Boundary Layer at Mach 5," NOLTR 72-33, Jan. 1972, Naval Ordnance Lab., White Oak, Md.

[54] Burbank, P. B., Newlander, R. A., and Collins, I. K., "Heat-Transfer and Pressure Measurements on a Flat-Plate Surface and Heat-Transfer Measurements on Attached Protuberances in a Supersonic Turbulent Boundary Layer at Mach Numbers of 2.65, 3.51 and 4.44," TN D–1372, Dec. 1962, NASA.

[55] Dean, W. R., "On the Shearing Motion of Fluid Past a Projection," *Proceedings of the Cambridge Philosophical Society*, Vol. 40, Pt. 1, March 1944, pp. 19–36.

[56] Dean, W. R., "Note on the Shearing Motion of Fluid Past a Projection," *Proceedings of the Cambridge Philosophical Society*, Vol. 40, Pt. 3, Oct. 1944, pp. 214–222.

[57] Gertsenshtein, S. Ya., "Effect of a Single Roughness Element on Turbulence Onset," *Mekhanika Zhidkosti i Gaza*, Vol. 1, No. 2, 1966, pp. 163–166; also *Journal of Fluid Dynamics*, Vol. 1, 1966, pp. 113–115 (Faraday Press Translation).

[58] Schubert, G., "Viscous Incompressible Flow Over Wall Projections and Depressions," *AIAA Journal*, Vol. 5, No. 2, Feb. 1967, pp. 373–375.

[59] Hunt, J. C. R., "A Theory for the Laminar Wake of a Two-Dimensional Body in a Boundary Layer," *Journal of Fluid Mechanics*, Vol. 49, Pt. 1, 1971, pp. 159–178.

[60] Libby, P. A. and Fox, H., "Some Perturbation Solutions in Laminar Boundary-Layer Theory," *Journal of Fluid Mechanics*, Vol. 17, Pt. 3, 1963, pp. 443–449.

[61] Fox, H. and Libby, P. A., "Some Perturbation Solutions in Laminar Boundary Layer Theory. Part 2. The Energy Equation," *Journal of Fluid Mechanics*, Vol. 19, Pt. 3, July 1964, pp. 433–451.

[62] Chen, K. K. and Libby, P. A., "Boundary Layers With Small Departures From the Falkner-Skan Profile," *Journal of Fluid Mechanics*, Vol. 33, Pt. 2, Aug. 1968, pp. 273–282.

[63] Chen, K. K., "Solutions to Nonsimilar Energy and Species Equations in Falkner-Skan Flows," *AIAA Journal*, Vol. 8, No. 1, Jan. 1970, pp. 39–43.

[64] Serrin, J., "Asymptotic Behavior of Velocity Profiles in the Prandtl Boundary Layer Theory," *Proceedings of The Royal Society*, Series A, Vol. 299, No. 1459, July 1967, pp. 491–507.

[65] Nee, V. W. and Kovasznay, L. S. G., "The Calculation of the Incompressible Turbulent Boundary Layers by a Simple Theory," *Proceedings on the Computation of Turbulent Boundary Layers—1968 AFOSR-IFP-Stanford Conference*, Vol. I, pp. 300–319.

[66] Hawthorne, W. R. and Martin, M. E., "The Effect of Density Gradient and Shear on the Flow Over a Hemisphere," *Proceedings of The Royal Society*, Series A, Vol. 232, 1955, pp. 184–195.

[67] Sedney, R., "Steady Three-Dimensional Perturbations in Boundary Layers," TR 71–25c, Nov. 1971, Research Institute for Advanced Study, Baltimore, Md.